

# Mechanical Properties and Wear Resistance of Semisolid Cast $\text{Al}_2\text{O}_3$ Nano Reinforced Hypo and Hyper-eutectic Al–Si Composites

I.S. El-Mahallawi and A.Y. Shash

**Abstract** The present investigation studies the prospects of using nanoparticles as reinforcement ceramic powders to gain improved performance of hypo and hyper eutectic Al cast alloys. A series of castings were prepared using A356 and A390 as the matrix alloy and alumina nano-powder in 40 nm size as the reinforcement. The nanoparticles were added to the molten slurries with stirring with different fraction ratios ranging from (0, 1, 2 and 4 wt%) in the mushy zone using a constant stirring time for one minute. To evaluate the results, the alloys were further characterized by various tribological and mechanical characterization methods. The results showed higher strength values with improved ductility compared to the monolithic alloys under the same casting conditions. The results also showed improvement in the wear resistance of the nano-reinforced alloys. The scanning electron microscopy of the fracture surface and the wear surface revealed the presence of nanoparticles in the interdendritic spacing and this confirmed with EDX analysis of these particles. The data obtained from the experimental work in this study together with previous published work by the authors were statistically analyzed using analysis of variance (ANOVA) to define the significant factors on both ultimate tensile strength and ductility and their level of confidence, using the orthogonal array L8. Response surface methodology (RSM) was used to build a model relating the type of matrix and nanoparticles addition to the ultimate tensile strength (UTS). The results have shown that the percent of the nanoparticles additions have a significant effect on the tensile properties of the alloys.

**Keywords** Nano-metal matrix composites •  $\text{Al}_2\text{O}_3$  nano-powders • Wear resistance • Mushy zone • Mechanical stirring

---

I.S. El-Mahallawi

Metallurgical Engineering Department, Faculty of Engineering, Cairo University,  
Giza, Egypt

e-mail: ielmahallawi@bue.edu.eg

A.Y. Shash (✉)

Mechanical Design and Production Department, Faculty of Engineering,  
Cairo University, Giza, Egypt

e-mail: ahmed.shash@cu.edu.eg

© Springer Science+Business Media Singapore 2017

A. Öchsner and H. Altenbach (eds.), *Properties and Characterization of Modern Materials*, Advanced Structured Materials 33,  
DOI 10.1007/978-981-10-1602-8\_2

## 1 Introduction

Composite materials are emerging chiefly in response to unprecedented demands from technology due to rapidly advancing activities in aircrafts, aerospace and automotive industries. These materials have low specific weight that makes their properties particularly superior in strength and modulus to many traditional engineering materials such as metals. Composite structures have shown universally savings of at least 20 % over metal counterparts and a lower operational and maintenance cost [1]. Aluminum based alloys and metal matrix composites (MMCs) exhibit attractive tribological and mechanical properties such as high specific modulus, good strength, long fatigue life, superior wear resistance and improved thermal stability, which allow these alloys to have numerous applications in the aerospace, automobile and military industries. The released data on the service life of composite structures shows that they maintain dimensional integrity, resist fatigue loading and are easily maintainable and repairable. Composites will continue to find new applications, but the large scale growth in the marketplace for these materials will require less costly processing methods and the prospect of recycling [2] will have to be solved [3].

As a result of intensive studies into the fundamental nature of materials and better understanding of their structure property relationship, it has become possible to develop new nanodispersed composite materials with improved physical and mechanical properties [4–8]. These new materials include high performance composites such as polymer matrix composites (PMCs), ceramic matrix composites (CMCs) and metal matrix composites (MMCs). Continuous advancements have led to the use of composite materials in more and more diversified applications. The importance of composites as engineering materials is reflected by the fact that out of over 1600 engineering materials available in the market today more than 200 are composites [6].

The challenge with manufacturing composite materials occurs in obtaining homogeneous distributions of the secondary phase which is usually a ceramic material. For most applications, a homogeneous distribution of the particles is desirable in order to maximize the mechanical properties [5, 7]. The manufacturing method also represents a challenge where researchers used both casting and powder metallurgy methods. Mechanical stir casting is a practical and economic method that has been used by researchers and industry to produce MMCs [4–8]. In order to achieve a good homogeneous distribution of a particle in the matrix, the process parameters related with the stir casting method were studied [4, 5, 7, 8]. The influence of stirring speed and stirring time on the distribution of the particles in MMCs has been investigated and Prabu [9] has recommended stirring speeds in the range of 500–700 rpm and the stirring times taken in the range 5–15 min.

Evidence of significant enhancement in strength and other properties of Al–Si cast alloys by incorporating nanoparticles have been recently presented, for example El-Mahallawi et al. [4–13] have shown that introducing  $\text{Al}_2\text{O}_3$  nano-ceramic particles to A356 and A390 alloys cast in the semi-solid state with

mechanical stirring has a beneficial effect on optimizing the strength–ductility relationship in these alloys. Mazahery et al. [10] used stir casting with a modified treatment for the added particles and have also shown significant improvement in hardness, 0.2 % yield strength, UTS and ductility of (A356) alloy. Rohatgi et al. [11] have predicted the significant role of producing Al–Si ceramic composites for bearings, pistons, cylinder liners, etc. leading to savings in materials and energy. Strengthening in nanostructured material is owed to having an appreciable fraction of their atoms in defect environments such as grain or interface boundaries [14].

Though previous studies have claimed enhanced mechanical properties for the rheocast and nanodispersed alloys relative to those produced by reinforcing with micro particles and conventional casting techniques [4–13], little work is done on evaluating the performance of these alloys related to real life applications [8, 15]. Therefore the aim of this research work is to evaluate the influence of the Al<sub>2</sub>O<sub>3</sub> nano particles dispersion on the mechanical and tribological properties of the A356 and A390 aluminum alloys cast in the semisolid state.

## 2 Experimental Procedures

The experimental work carried out through this scientific study consists of the following three stages:

- (a) Production of the new NMMC alloys.
- (b) Identification of the mechanical and wear resistance properties.
- (c) Characterization of the new material.

### 2.1 Materials Produced

The hypoeutectic alloy A356 and the hypereutectic A390 alloy were used as a base metal for the produced material having the following chemical composition illustrated in Table 1. The material used for reinforcement was 1, 2, and 4 % by weight Al<sub>2</sub>O<sub>3</sub> ceramic nano-particles with constant particle size of 40 nm, (provided by Nano-Tech Egypt), the description of which is given in Table 2.

**Table 1** Chemical composition (in wt%) of A356 cast Al–Si

Alloy	Chemical Composition (wt%)								
	Al	Si	Mg	Fe	Cu	Pb	Ti	Zn	Mn
A356	Bal.	7.44	0.3	0.27	0.02	0.022	–	0.01	Nil
A390	Bal.	17	0.45	0.5	4.5	–	0.2	0.1	0.1

**Table 2** Properties of  $\text{Al}_2\text{O}_3$  reinforcement powders

Reinforcement	$\gamma\text{-Al}_2\text{O}_3$
Density (solid) ( $\text{g/cm}^3$ )	3.95
Crystal structure	FCC
Appearance	White solid
Young's Modulus (GPa)	380
Average size (nm)	40
Melting point	2054 °C

## 2.2 Casting and Composite Manufacturing

### 2.2.1 Melting Furnace

An electric resistance furnace was designed and constructed for approaching this research work for preparing the NMMCs. It consists of a lift out ceramic crucible up to 5 kg, heating system, and is connected to a stirring mechanism with 3000 rpm max. rotating speed motor and adjustable height with a control unit up to 1200 °C connected to a thermocouple for controlling the stirring temperature as illustrated in Fig. 1.

### 2.3 Melting Methodology and Approach

A charge of 0.5 kg of the A356 alloy was introduced to the crucible and heated up to the melting temperature (640 °C). The melt was degassed and shielded with argon before pouring after reaching the liquid state to prevent oxidation of the molten metal. The melt was subsequently brought down to the semi-solid state by around 605 °C and hence the  $\text{Al}_2\text{O}_3$  nano- powders were preheated to 700 °C and then added to the melt simultaneously with mechanical stirring for 1 min at 1500 rpm. The fabrication conditions of the composites prepared in this

**Fig. 1** Schematic apparatus used for preparing the NMMCs

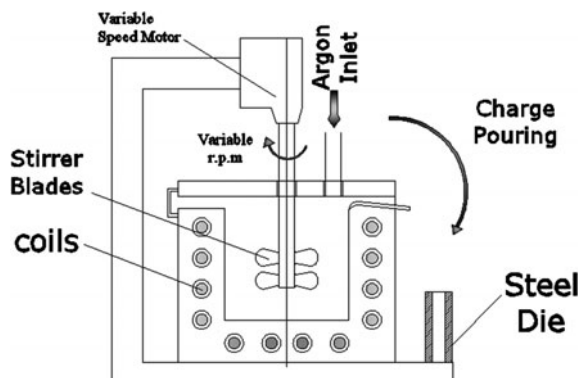


**Table 3** List of produced alloys and fabrication conditions

Melt No.	Additions	Stirring (rpm)	Pouring Temp. (semi-solid) (°C)
Melt 1	A356	1500	605
Melt 2	A356 + 1 % $\text{Al}_2\text{O}_3$	1500	605
Melt 3	A356 + 2 % $\text{Al}_2\text{O}_3$	1500	605
Melt 4	A356 + 4 % $\text{Al}_2\text{O}_3$	1500	605
Melt 5	A390	1000	660
Melt 6	A390 + 2 %	$\text{Al}_2\text{O}_3$	660

investigation are summarized in Table 3. Cast samples were poured in the prepared mould without additions and with additions of the different investigated  $\text{Al}_2\text{O}_3$  percentage.

Similarly, 3 kg charge of the hypereutectic base alloy was introduced to the crucible and heated up to above the melting temperature (730 °C). After reaching the liquid state the melt was degassed with either argon or hexachlorethane degasser tablet, to get rid of gases. After degassing the melt was brought down to 660 °C, and poured. 2 %  $\text{Al}_2\text{O}_3$  nanoparticles were prepared in packages of aluminium foil and preheated to about 600 °C, added at 660 °C, stirred for 1 min and poured. The packets were added to the melt through the opening in the top of the furnace one packet after the other, simultaneously with mechanical stirring for 1 min at 1000 rpm.

## 2.4 Mechanical Properties

Mechanical properties, mainly tensile strength, ductility, hardness and wear resistance were determined in the as-cast conditions for the investigated NMMC samples.

### 2.4.1 Tensile Test

The tensile tests were conducted on round tension test specimens of diameter 5.02 mm and gage length 25.2 mm using a universal testing machine according to DIN 50125. The elongation percent and ultimate tensile strength were calculated. The results were based on the average of three samples taken from each melt.

### 2.4.2 Hardness Test

The overall hardness of the A356 composite was measured by a Rockwell hardness testing machine, using a  $\left(\frac{1}{16}\right)''$  diameter hardened steel ball and a 62.5 kg applied load.

As for the A390 composite material, a Brinell hardness testing machine using 2.5 mm diameter hardened steel ball and 1839 N applied load was used. The reported results are the average of three reading for each case.

### **2.4.3 Wear Test**

A PLINT TE 79 multi axis tribometer machine was used for measuring the friction force; friction coefficient and wear rate for NMMC manufactured materials. In which a standard specimen with diameter of 8 mm and 20 mm length as a computerized pin on disc machine used for Friction and wear testing of materials is loaded vertically downwards onto the horizontal disc. The wear tests were then performed for the A356 composite material with the following parameters: velocity = 0.8 m/s, time = 1200 s and load = 10 N. The differences in the weight of the samples were taken as an indication of the wear resistance of the material.

The wear test conditions for the A390 composite material is presented elsewhere [7].

## **2.5 Material Characterization**

### **2.5.1 Microstructural Study**

Representative sections from the cast samples were cut into 3 pieces: the 1st from the top, the 2nd from the middle and the 3rd from the bottom. Samples were wet grounded on a rotating disc using silicon carbide abrasive discs of increasing fineness (120, 180, 220, 320, 400, 600, 800, 1000 and 1200 grit). Then they were polished using 10  $\mu\text{m}$  alumina paste.

### **2.5.2 Optical Microscopy (OM)**

The microstructure examination was carried out using an OLYMPUS DP12 optical metallurgical microscope, equipped with a high resolution digital camera for microstructural investigations.

### **2.5.3 Scanning Electron Microscopy (SEM)**

The surface topography and fracture characteristics were studied using SEM to understand the fracture mechanism and also to detect the favorable sites for particle incorporation in the Gemeinschaftslabor fuer Metallographie, RWTH-Aachen University by using a JSM-5410 and JSM-7000F FEG-SEM. Both microscopes are high-performance multipurpose SEM with a high-resolution of 3.5 nm, and EDXS

(energy dispersive X-ray spectrometer), with automated features including auto focus/auto stigmator, and automatic contrast and brightness. The EDS expands the function from morphological observation to multi-purpose high-resolution elemental analysis.

## 2.6 Statistical Analysis

Statistical analysis by using ANOVA was used to find the significant factor affecting on tensile strength. The data used was based on the experimental data obtained from this work, in addition to previous work by the authors [4–8]. Material type (Si content), pouring temperature and nanoparticles percent were the factors used in the orthogonal array L8 and the ultimate tensile strength (UTS) and the elongation % were the response.

## 3 Results

### 3.1 Mechanical Properties of the NMMC

Figures 2 and 3 illustrate the mechanical properties (tensile strength, elongation% and hardness) of the produced castings with reinforced  $\text{Al}_2\text{O}_3$  nanoparticles in A356 and A390 metal matrix, respectively.

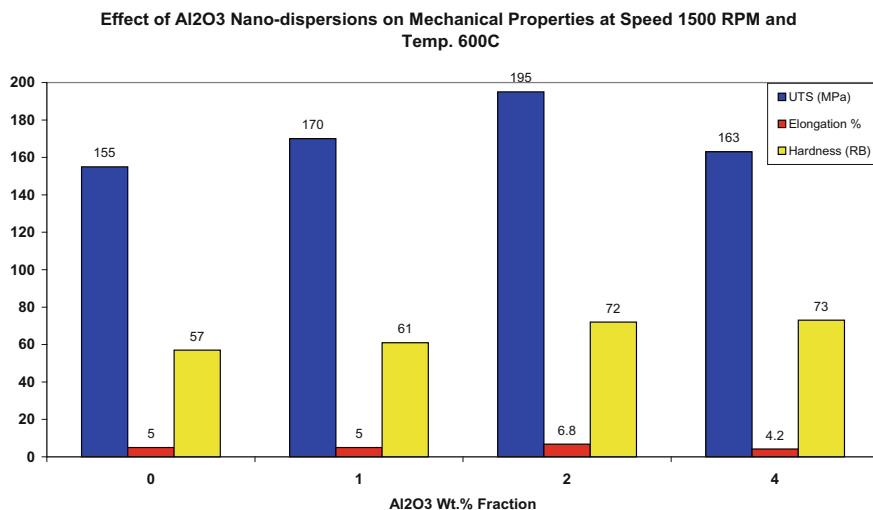


**Fig. 2** The effect of wt% fraction of  $\text{Al}_2\text{O}_3$  nano-powders in A356 on the UTS, elongation % and Hardness of MMC at 1500 rpm stirring speed at semi-solid state (600 °C)

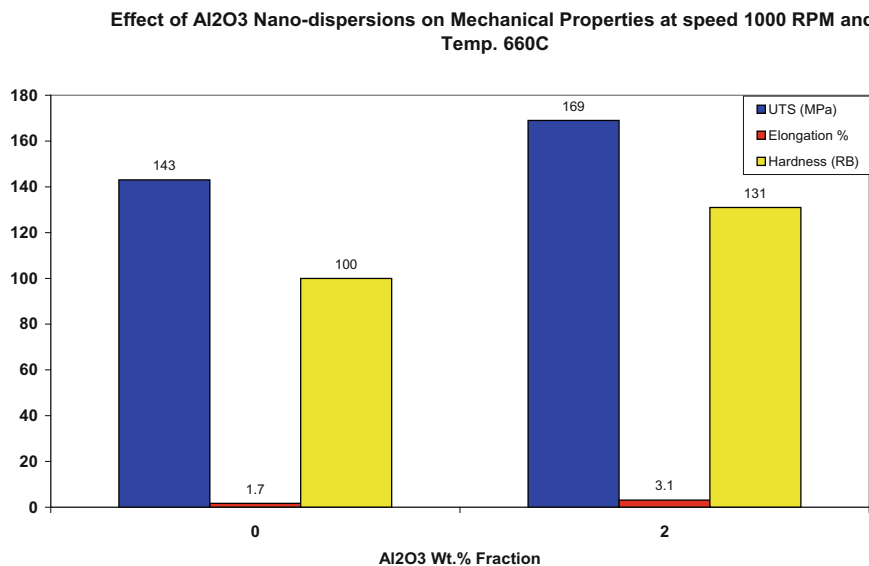


**Fig. 3** The effect of 2 wt% of Al<sub>2</sub>O<sub>3</sub> nano-powders in A390 on the UTS, elongation % and Hardness of MMC at 1000 rpm stirring speed at semi-solid state (660 °C)

It is shown in Fig. 2 that as the fraction of Al<sub>2</sub>O<sub>3</sub> nanopowder (wt%) increases, up to a value of 2 wt% of Al<sub>2</sub>O<sub>3</sub>, the UTS increases reaching 195 MPa. Beyond this weight fraction, the UTS decreases as the wt% increases. As shown in Fig. 2, increasing the weight fraction of Al<sub>2</sub>O<sub>3</sub> has no visible effect on ductility until reaching 1 wt%, then with increasing the wt% beyond 1 wt% the ductility increases. The ductility of NMMC increases by about 40 % at 2 wt% of Al<sub>2</sub>O<sub>3</sub> nanoparticles. At 4 wt% fraction, the ductility reaches its minimum values; probably due to the agglomeration of the dispersed particles in the NMMC, while its hardness at this weight fraction increases by about 30 % as shown in Fig. 2. The presence of the ceramic agglomerates increases the hardness of the alloys and hence, reduces the ductility of the composites in comparison with the matrix alloy.

The enhanced strength properties along with good ductility which are observed in these alloys (with 1 and 2 wt% nanoparticles) probably originate from the fine distribution of globular particles in an A356 matrix on a nanometer scale, where the globular particles act as strength bearing components, while the A356 matrix supplies ductility. The existence of a crystalline approximant phase at the interface between the particles and the FCC Al matrix improves interfacial bonding between the different phases, leading to the combination of high strength and good ductility without failure at the interface [13].

Similar results were obtained for the A390 composite alloy where an increase of 18 % occurred in the tensile strength and 82 % in the ductility and 31 % in the hardness after adding 2 wt% nanoparticles.



The observed increase in the hardness of the A356 and A390 nano-reinforced alloys suggests a misfit effect in the lattice parameter of the matrix phase, due to cooling induced changes caused by the difference between the coefficients of thermal expansion between the primary phase (Al or Si) and the nanoparticles: ( $3 \times 10^{-6}$  m/m K, for Si and  $5.4 \times 10^{-6}$  for  $\text{Al}_2\text{O}_3$  nanoparticles), resulting in an increase in the hardness of the first. Additionally, enhanced dislocation generation and reduced sub grain size owing to the presence of the nanoparticles may be contributing to the increased hardness for the aluminium phase.

### 3.2 Statistical Analysis

ANOVA technique was applied on the responses to find the factors (f) and compare it with the tabulated values at the levels of confidence (90, 95, and 99 %). Response surface methodology (RSM) is the technique used to build models to correlate the responses and factors. Table 4 shows the orthogonal array L8 that was used to apply the ANOVA technique.

The obtained results showed that nano-reinforcement is significant at 99 %. The silicon content (type of alloy) is significant at 95 %.

The Anova analysis has shown that the following equations may be used to predict the mechanical properties of nano-reinforced AlSi alloys:

$$\text{UTS} = \text{UTS (monolithic alloy)} + 14 \times \text{Nano\%} - 0.57 \text{ stirring temp} + 0.0383 \times (\text{Si} \times \text{semi-solid temp})$$

$$\text{Elongation \%} = \text{Elongation \% (monolithic alloy)} + 0.5812 \times \text{Nano\%} - 0.0561 \times \text{semisolid temp} + 0.0042 \times (\text{Si} \times \text{semi-solid temp})$$

Figure 4 shows the comparison between the UTS and elongation % predicted by these equations and the measured values for the experimental alloys prepared in this work.

### 3.3 Microstructure Study

Figure 5a, b shows the optical microstructure of the base matrix A356 alloys reinforced with 2 wt% fraction of  $\text{Al}_2\text{O}_3$  nano-powder. Also, the optical microstructure

**Table 4** Factors levels for ANOVA Analysis

Factor	Level 1	Level 2
Si%	0	2
Nanoparticle%	0	2
Semi-solid pouring temp	0	2

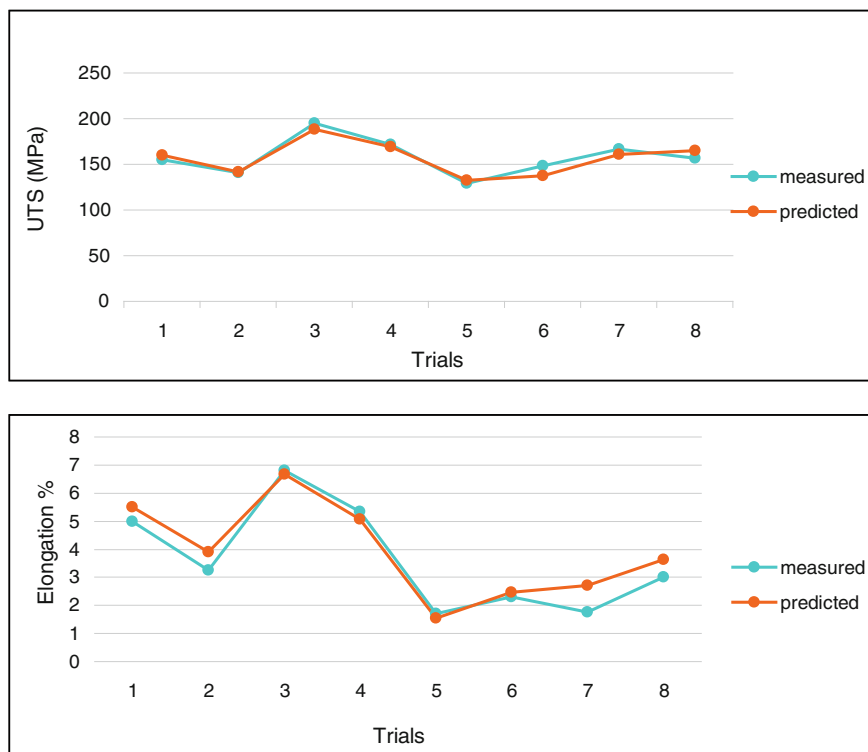


**Fig. 4** Comparison between measured and predicted data for UTS and Elongation %

of the base matrix A390 alloys reinforced with 2 wt% fraction of  $\text{Al}_2\text{O}_3$  nano-powder is shown in Fig. 6a, b. The microstructures of the two castings show that the phases in A356 are uniformly distributed consisting of primary aluminium and eutectic structure, whereas it includes primary Si particles too in the A390 composite material. It also shows clearly a morphological change in the microstructures. In the base matrix sample, the microstructure is dendritic whereas in the other rheocast samples, some of the primary dendrites change to globular structures due to mechanical stirring.

As the structure contains good amount of eutectic phases it should give a range of mechanical properties when mechanical stirring processed [7, 14]. This was clear in the mechanical properties of alloys reinforced with nano-powder using mechanical stirring. It was also observed from the metallographic pictures and applying image analyzer technique that by increasing the stirring speed and the quantity of nano-dispersions, the eutectic phases would decrease by around 10 %.

The SEM illustrated in Figs. 7 and 8 show a typical fracture surface for a specimen reinforced with 2 wt% fraction of  $\text{Al}_2\text{O}_3$  in A356 and A390, respectively. The fracture surface shows a mixture of dendrites and globular structures. Agglomerated nanoparticles also appear. The agglomeration could happen by the

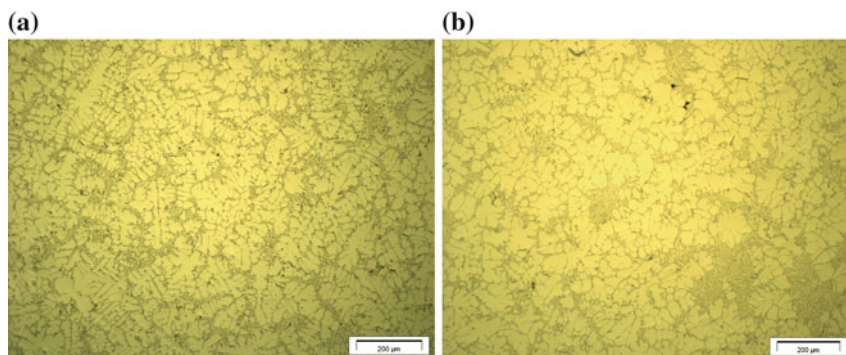


**Fig. 5** The optical microstructure of **a** Base matrix A356 alloys **b** Reinforced with 2 wt% fraction of  $\text{Al}_2\text{O}_3$  nano-powders

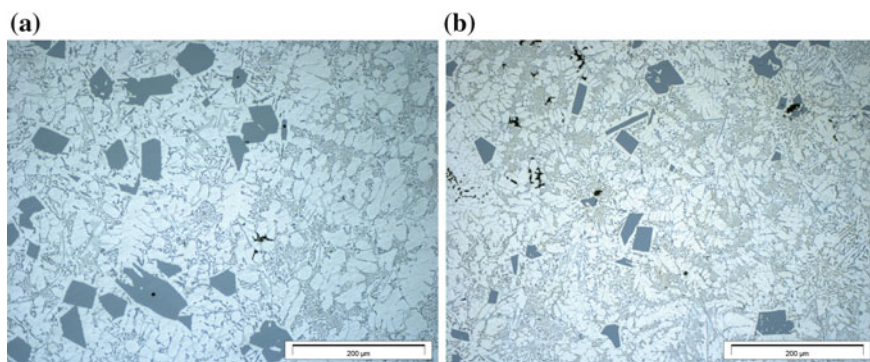


**Fig. 6** The optical microstructure of **a** Base matrix A390 alloys **b** Reinforced with 2 wt% fraction of  $\text{Al}_2\text{O}_3$  nano-powders

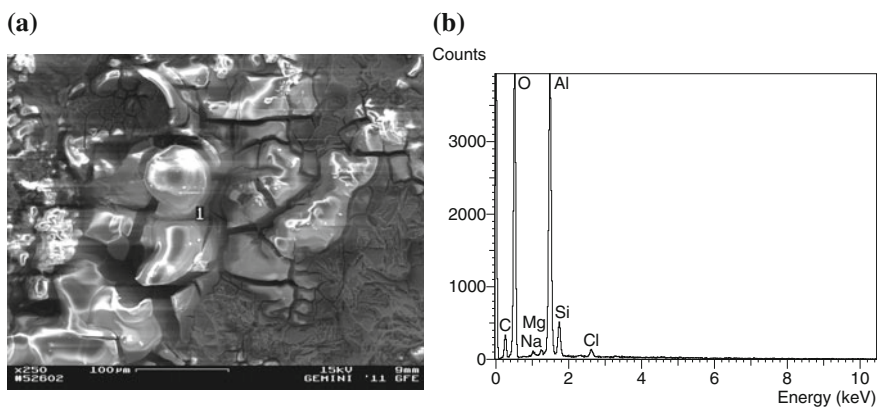


**Fig. 7** **a** SEM of the fracture surface A356 specimen reinforced with 2 %wt fraction of  $\text{Al}_2\text{O}_3$  nano-powder. **b** EDX of  $\text{Al}_2\text{O}_3$  agglomerated particles

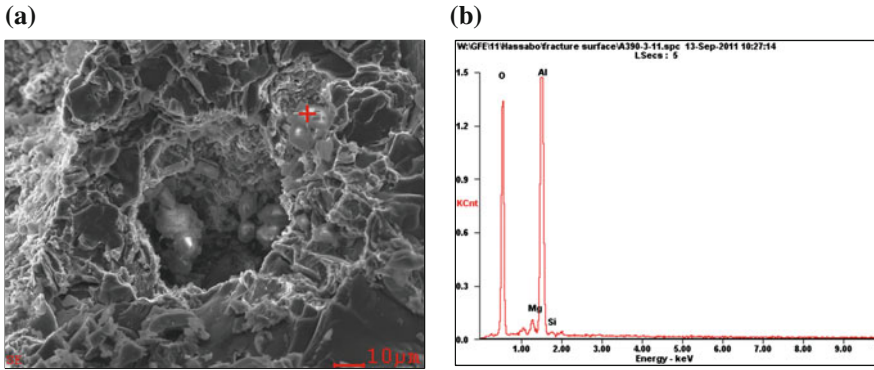


**Fig. 8** **a** SEM of the fracture surface A390 specimen reinforced with 2 %wt fraction of  $\text{Al}_2\text{O}_3$  nano-powder. **b** EDX of  $\text{Al}_2\text{O}_3$  agglomerated particles

**Table 5** Specified analysis of the EDX of  $\text{Al}_2\text{O}_3$  agglomerated particles

Label	Range (keV)	Gross	Net	Total %
O Ka	0.407–0.668	5459	3149	38.1
Al Ka	1.327–1.628	5942	4222	51.1
Si Ka	1.648–1.888	2347	891	10.8

particles reinforced inside the matrix during the melting stage. Moreover, these agglomerated particles were not homogenously distributed inside the matrix.  $\text{Al}_2\text{O}_3$  agglomerated particles have a size less than  $1\ \mu\text{m}$  attached in the interdendritic space for the A356 composite alloy and bonded to the primary Si particles for the A390 composite alloy. The EDX analysis shown in Figs. 7b and 8b, has evidently confirmed that these are  $\text{Al}_2\text{O}_3$  particles though a strong reflection from the matrix was inevitable. The specified analysis of the EDX and the percentage of O, Al and S are illustrated in Table 5. It is clear that the high percentage of the oxygen and aluminum, confirms the presence of  $\text{Al}_2\text{O}_3$  nano-powders in the matrix.

The fracture surface of the nano-dispersed hypereutectic alloys agrees with previous findings [13] and shows that the major mechanism of fracture is the breakage of the faceted Si particles and the debonding at the interfaces between Al phase and Si particles, where the crack crosses the cleavage planes in the primary Si particles round with the eutectic Al and Si regions. The nano-particles adhere themselves to the primary Si particles in several locations (whereas in the case of the hypoeutectic alloy A356 they were found in interdendritic locations). This is explained in view of the solidification effective mechanisms for both cases where dendrite growth in the process of solidification tends not to include the impurity into the crystal, but to push the oxide nano-particles and the impurity into the residual melt [16]. On the other side, in the case of equiaxed structures a part of remained

**Table 6** Average wear results of A356 samples reinforced with 0, 1, 2 and 4 wt%  $\text{Al}_2\text{O}_3$  nanopowder

Sample no.	Additions	Weight loss (mg)	Friction coefficient
1	A356	3.9	0.4
2	A356 + 1 % $\text{Al}_2\text{O}_3$	4.0	0.361
3	A356 + 2 % $\text{Al}_2\text{O}_3$	4.5	0.385
4	A356 + 4 % $\text{Al}_2\text{O}_3$	5.5	0.430

liquid including oxide nano-particles is blocked inside the grain attaching themselves to the primary silicon particles [8, 16].

### 3.4 Results of Wear Test

The average wear results of A356 samples reinforced with 0, 1, 2 and 4 wt%  $\text{Al}_2\text{O}_3$  nanoparticles are shown in Table 6. It can be seen from Table 6 that the addition of 1 % nanoparticles resulted in a significant drop in the friction coefficient, unaccompanied with any improvement in terms of weight loss. Increasing nanoparticles up to 4 % resulted in a deterioration in the wear resistance in terms of friction coefficient and weight loss.

The results show that the addition of 1 % nano-particles did not produce a significant change on the wear resistance of the hypo-eutectic alloy A356, though there was a reduction in the friction coefficient. The fact that the wear resistance deteriorated after adding 2 and 4 % nanoparticles (though the hardness and strength increased) may be attributed to microstructural effects as well as the high load used in the test. Previous work by the authors on A390 alloy [7] has shown that the wear resistance of nano reinforced A390 was enhanced compared to monolithic A390 alloy, which has been attributed to higher hardness resulting from refinement in microstructural constituents. The main wear mechanism observed [7] was delamination and tearing. Other work [15] has reported enhancement in the wear resistance of A356 rheocast alloy compared to those obtained by conventional casting, which has been attributed to the equiaxed structure obtained by rheocasting. The main wear mechanism was found to be ploughing at small stresses and mixed ploughing and delamination at high stresses. However, no data has been found to evaluate the wear performance of the rheocast nanodispersed A356 alloy.

The samples subjected to wear tests have been examined using SEM. Figure 9a, b shows clearly the  $\text{Al}_2\text{O}_3$  nano-particles distributed on the surface of samples with 1 and 4 wt%  $\text{Al}_2\text{O}_3$  addition subjected to wear, respectively. The figure also shows that the dominant wear mechanism was a combination of adhesion and delamination mechanisms, similar to findings in a previous work for hypereutectic AlSi alloy A390 [7].

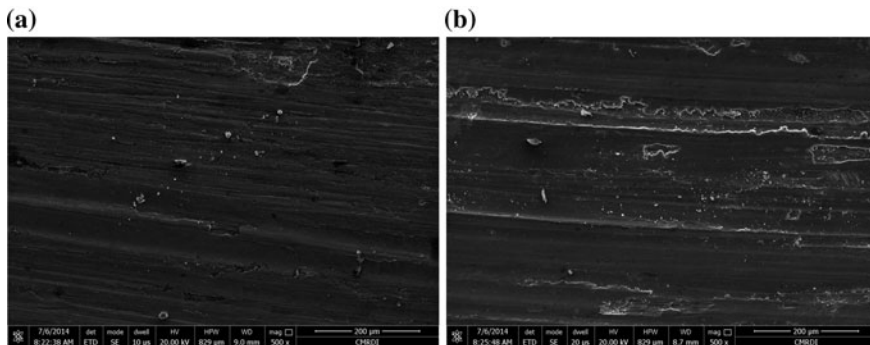


**Fig. 9** SEM image for wear surface of **a** 1wt%  $\text{Al}_2\text{O}_3$  and **b** 2 wt%  $\text{Al}_2\text{O}_3$  nano-particles

The nano-composites manufactured using the semi-solid route exhibited better mechanical properties when compared with those prepared by the liquid metallurgy rout. Also, a high mixing speed is required in order to obtain a good distribution of the particles reinforced and to introduce it inside the matrix as introducing the reinforced  $\text{Al}_2\text{O}_3$  particles to the A356 matrix in the semi solid state is difficult due to the higher density of the matrix at this state, in which the alloys stirred with 1500 rpm exhibits the best tensile strength and elongation.

The A356 matrix alloy reinforced with 2 wt% fraction of  $\text{Al}_2\text{O}_3$  nano-powder has the best tensile strength properties at conditions of 1500 rpm stirring speed at semi solid state temperature 600 °C. The wear resistance increases as the weight percentage of the reinforced nano-particles increases. The wear resistance results were evidently confirmed by increasing the hardness and decreasing the friction coefficient values as the wt% of the nano-dispersions increases.

In the base matrix sample without stirring, the microstructure is dendritic whereas in the other rheocast samples, the primary dendrites are fragmented due to mechanical stirring which explains the improvement in the mechanical properties. Analysis using both scanning electron microscope and high magnification shows evidence for the possibility of incorporating and entrapping nano-sized particles within the interdendritic interface developing during the solidification of the dispersed alloys.

## 4 Discussions

Rapid quenching from the melt or solid state reaction have been identified as processing routes for obtaining nanostructured materials leading to two phase nanostructures, however, it is highly desirable to obtain such nanostructures directly in bulk form, e.g. through casting [14]. The current work focuses on the properties of nanodispersed A356 and A390 alloys obtained by rheocasting, which is a

challenging production method for producing nanodispersed alloys. The potential for nanodispersed materials for being high-tech material has been explored [16] and it has been shown that the addition of nano oxides results in the improvement in both the hardness and the tensile strength of stir cast aluminium, which has been explained by the tendency of oxide nanoparticles to agglomerate at the grain boundaries in the columnar structures, whereas these oxide nanoparticles are uniformly dispersed in the equiaxed structure resulting from stirring.

The difference between the wear performance of the nanodispersed hypo and hyper eutectic alloys (reported in this work) may be explained by the effect of the nano particles additions on both alloys. The addition of nanoparticles promotes the formation of the  $\alpha$ -Al phase and has been attributed to the improved nucleation of Si particles and depletion of Si element near the Si particles [8, 17]. This would produce a deterioration effect on the wear resistance of the hypo-eutectic alloys, whereas the effect would be less significant on the hyper-eutectic alloys, since the morphology of the Si particles and the shape of the  $\alpha$ -Al, as well as the morphology of the eutectic Si have a major contribution. It has been stated [17] that the cracks easily initiate inside the brittle primary Si or eutectic Si, and then propagate through boundaries with  $\alpha$ -Al phase, thus the change in the Si morphology (according to restricted nucleation and growth theory of modification), and the crystalline appearance of the  $\alpha$ -Al phase would improve the wear resistance for the hyper-eutectic alloys [8]. Also, the addition of nanoparticles to the hypereutectic alloys has been shown to produce a refining effect on the primary silicon particles, which has been attributed to increasing the nucleation sites [17] or inducing a thermal sub-cooling effect.

It has been shown [4–8] that nanodispersed aluminium alloys have refined microstructural constituents (Al dendrites, interlamellar spacing and primary Si particles) compared to their monolithic counterparts. The mechanical strength of crystalline metals or alloys is largely controlled by the grain size “d”. The well known empirical Hall–Petch equation relates the yield strength “ $\sigma_y$ ” to the average grain size “d” according to  $\sigma_y = \sigma_0 + k d^{-1/2}$ . Where  $\sigma_0$  is the friction stress and k is a constant. A similar relation exists between the hardness and the grain size. Consequently, reducing “d” to the nanometer regime increases the strength considerably. However, the limits of the conventional description of yielding and of new mechanisms that may occur at these small dimensions need to be explored and studied in much more detail [14].

Nanodispersed cast structures carry both natures of composites and refined structures. It is important at this stage to understand the active strengthening mechanisms in these materials as this will be the key to develop new structures.

The known models addressing the incorporation of particles into a solidifying matrix have been identified [18] to be: (i) the kinetic models based on the interaction between the velocity of the solid/liquid interface and the velocity of the particle, (ii) the thermodynamic models which are closely related to classical heterogeneous nucleation theory and (iii) the models based on the ratio of the thermophysical properties of the particles and the melt. A good correlation among all three models [19] has integrated many of the effective parameters and has



suggested that there are three possible pathways for nanoparticle capture: viscous capture, Brownian capture and spontaneous capture. Viscous capture occurs under conditions of extremely high cooling rates or increased viscosity of the melt. Brownian capture is likely to occur when the nanoparticles have slightly lower Hamaker constants than the melt. Spontaneous capture was proposed as the most favorable for nanoparticle capture during solidification of metal melt, the key being to select or design/fabricate suitable nanoparticles that offer a higher Hamaker constant than that of the liquid metal [19]. However, the problem with these models is that they consider capturing of the nanoparticles but ignore strengthening mechanisms for the proposed matrix/reinforcement combinations.

This work and other work have shown that adding nanoparticles to metal matrix composites (A356 and A390 in this case) has significant potential of enhancing both strength and ductility. The addition of ceramic particles to aluminium alloys raises the viscosity very quickly [20] providing suitable conditions for particle capture, moreover the  $\text{Al}_2\text{O}_3$  nanoparticles have been shown to possess appropriate properties that are compatible with the Al alloy, namely relatively high thermal conductivity and thermal expansion coefficients that affects its role as a nanodispersion for reinforcement in the Al alloy matrix [4–8]. It has been shown [20, 21] that in eutectic and hypereutectic matrix alloys, such as Al-Si, particle capture take place for all growth conditions, whereas, in hypoeutectic Al alloy systems, where a non-planar solid-liquid interface is typically present, particle pushing takes place. The classical theory for strengthening in dispersed structures forming composites [17, 20, 21] is based on the dislocation motion being constrained by the precipitates and dispersoid particles. These particles form coherency strains and dislocation networks around them, leading to a misfit between the particles and the matrix which causes the hardness and strength to increase. The usual drop in ductility associated with increase in strength is explained by the fact that dislocations move on specific slip planes under the action of a shear stress. If the slip plane has obstacles penetrating it, e.g., precipitates or dispersoids, a dislocation moving on this slip plane must interact with these obstacles. The high volume fraction of interfacial regions offered by the nanodispersion causes the improvement in ductility where grain boundary sliding becomes the major deformation mechanism [14].

## 5 Conclusion

1. The introduction of 2 % nano-sized particles leads to an increase in the hardness of the A356 alloy from about 57 HB to 72 RB, the tensile strength from 155 to 195 MPa, and the elongation% from 5 to 6.8 %; and the increase in the tensile strength of A390 alloy from 143 to 169 and the elongation % from 1.7 to 3.1 and the hardness from 100 to 131 HB.
2. The addition of nano particles promote the formation of Al phase and decrease in the amount of eutectic structure.



3. The introduction of varying amounts of nano-sized particles to the A356 alloy did not produce a significant change on the wear resistance of the tested hypo-eutectic alloy A356 material with 1 % nanoparticles and resulted deterioration after adding 2 and 4 % nanoparticles, though a drop in the friction coefficient occurred at 1 % addition [17]. While, the wear resistance of nano reinforced A390 was enhanced compared to monolithic A390 alloy after adding 1 % nanoparticles. This behavior is attributed to microstructural effects in both alloys, where nano additions promote Al phase formation for the hypoeutectic alloys, whereas their refining effect is more pronounced for the hypereutectic alloys.
4. It is possible to predict the UTS and elongation % of nanodispersed composite materials using equations developed by ANOVA analysis. These equations show that nanoparticles addition up to 2 % and the semisolid pouring temperature are the main controlling parameters.
5. Nanoparticles are pushed to interdendritic locations during the solidification of hypoeutectic AlSi alloys systems, and tend to adhere to primary Si particles during the solidification of hypereutectic alloys.

**Acknowledgement** The authors would like to acknowledge the role of late Prof. Dr.-Ing. Y. Shash the head of Mechanical Design and Production Dept., Faculty of Engineering, Cairo University who advised and supported this work at its early stages. Great thanks go also for Dr. M. El-Saeed, Eng. M. Hassabo and Eng. A. Abdel-Fatah for offering data to this scientific work.

## References

1. Dhingra A (1986) Metal replacement by composite. JOM 38(03):17
2. Mehrabian R, Riek R, Flemings M (1974) Preparation and casting of metal-particulate non-metal composites. Metall Trans 5A:1899–1905
3. Eliasson J, Sandstorm R (1995) Applications of aluminium matrix composites. Part 1, Newaz GM, Neber-Aeschbacherand H, Wohlbier FH (eds). Trans. Tech. publications, Switzerland, pp 3–36
4. El-Mahallawi I, Eigenfeld K, Kouta F, Hussein A, Mahmoud T, Rashad R, Shash A, Abou-AL-Hassan W (2008) Synthesis and characterization of new cast A356/ (Al<sub>2</sub>O<sub>3</sub>) p metal matrix nano- composites. In: Proceedings of the 2nd multifunctional nanocomposites & nanomaterials: international conference& exhibition MN2008, 11–13 Jan 2008, Cairo Egypt. Copyright © by ASME
5. El-Mahallawi I, Shash Y, Eigenfeld K, Mahmoud T, Rashad R, Shash A, El Saeed M (2010) “Influence of nano-dispersions on strength ductility properties of semi-solid cast A356 Al alloy. Mater Sci Technol 26(10):1226–1231
6. El-Mahallawi I, Abdelkader H, Yousef L, Amer A, Mayer J, Schwedt A (2012) Influence of Al<sub>2</sub>O<sub>3</sub> nano-dispersions on microstructure features and mechanical properties of cast and T6 heat-treated AlSi hypoeutectic alloys. Mater Sci Eng A A556:76–82
7. El Mahallawi I, Shash Y, Rashad R, Abdelaziz M, Mayer J, Schwedt A (2014) Hardness and wear behaviour of semi-solid cast A390 alloy reinforced with Al<sub>2</sub>O<sub>3</sub> and TiO<sub>2</sub> nanoparticles. Arab J Sci Eng 39(6):5171–5184
8. El Mahallawi I, Othman O, Abdelaziz M, Raed H, Abd El-Fatah T, Ali S (2014) Understanding the role of nanodispersions on the properties of A390 hyper-eutectic Al-Si cast alloy. TMS Light Metals 1361–1365

9. Prabu S (2006) Influence of stirring speed and stirring time on distribution of particles in cast MMC. *J Mater Process Technol* 171:268–273
10. Mazahery A, Baharvandi H, Abdizadeh H (2009) Development of high performance A356-nano  $\text{Al}_2\text{O}_3$  composites. *Mater Sci Eng A* 518:23–27
11. Rohatgi K, Asthana R, Das S (1986) Solidification, structure and properties of cast metal-ceramic particle composites. *Int Metals Rev* 31(3):115–139
12. Zhao J, Wu S (2010) Microstructure and mechanical properties of rheo-diecasted A390 alloy. *Trans Nonferrous Met Soc China* 20:754–757
13. Choi H, Konishi H, Li X (2012)  $\text{Al}_2\text{O}_3$  nanoparticles induced simultaneous refinement and modification of primary and eutectic Si particles in hypereutectic Al–20Si alloy. *Mater Sci Eng A* 541:159–165
14. Koch C (2002) Nanostructured materials processing, properties and potential applications, pp 423–526
15. Dey A, Poddar P, Singh K, Sahoo K (2006) Mechanical and wear properties of rheocast and conventional gravity die cast A356 alloy. *Mater Sci Eng A* 435–436:521–529
16. Kim G, Hong S, Lee M, Kim S, Ioka I, Kim B, Kim I (2010) Effect of oxide dispersion on dendritic grain growth characteristics of cast aluminum alloy. *Mater Trans* 51(10):1951–1957
17. El-Mahallawi I, Shash A, Amer A (2015) Nanoreinforced cast Al-Si alloys with  $\text{Al}_2\text{O}_3$ ,  $\text{TiO}_2$  and  $\text{ZrO}_2$  nanoparticles. *J Metals* 5(2):802–821
18. Boostani A, Tahamtan S, Jiang Z, Wei D, Yazdani S, Azari Khosroshahi R, Taherzadeh Mousavian R, Xu J, Zhang X, Gong D (2014) Enhanced tensile properties of aluminium matrix composites reinforced with graphene encapsulated SiC nanoparticles. *Composites: Part A*
19. Xu J, Chen L, Choi H, Li X (2012) Theoretical study and pathways for nanoparticle capture during solidification of metal melt. *J Phys Condensed Matter* 24:255304 (10 pp)
20. Chawla K (2006) *METAL MATRIX COMPOSITES*. Springer, Berlin
21. Shash A, Amer A, El-Saeed M (2015) “Influence of  $\text{Al}_2\text{O}_3$  nano-dispersions on mechanical and wear resistance properties of semisolid cast A356 Al alloy”, mechanical and materials engineering of modern structure and component design. *J Adv Struct Mater* 70:13–24 (Springer International Publishing)

Properties and Characterization of Modern Materials

Öchsner, A.; Altenbach, H. (Eds.)

2017, X, 452 p. 339 illus., 222 illus. in color., Hardcover

ISBN: 978-981-10-1601-1